3. METHOD

3.1 Determining Tortuosity

For this study, the transport of gaseous compounds through the soil cover layer was assumed to be dominated by diffusion. Advective movement caused by barometric pumping was not included in the study. The decision to ignore barometric effects was based on research by Buckingham (1904), Thibodeaux (1982), Nilson et al. (1991), Massman and Farrier (1992), and Auer et al. (1996). All but Auer et al. (1996) claim that in unfractured media, transport effects because of barometric pumping are small compared to diffusion. Auer et al. (1996) contends that barometric pumping can be important but it is highly dependent on properties of the system. In terms of actual numbers, the study by Thibodeaux (1982) found that barometric pumping enhanced emissions by 13% over diffusion alone. For the purposes of this study, errors of this magnitude were acceptable when measured against the additional effort required to address barometric pumping.

Another important finding of barometric pumping researchers (Buckingham 1904; Auer et al. 1996) is that barometric pressure changes do not significantly affect the rate of diffusion. Stated differently, diffusion would proceed at the same rate as when there is no air displacement because of barometric pumping. The diffusion rate is stable because even though barometric pumping moves gases up and down, the subsurface concentration gradients that control diffusion remain relatively constant.

Gas diffusion can be described by Fick's first law (Arah and Ball 1994), which states that the diffusive flux across a surface is proportional to the concentration gradient through a constant called the diffusion coefficient:

$$F = D * C_g \tag{1}$$

where

F = areal mass flux rate ($m/L^2/t$)

D = effective diffusion coefficient (l^2/t)

C_g = concentration gradient (Δ concentration/Δ depth) (m/L^4).

For a porous medium, the gaseous molecules must travel longer diffusion paths because of the structure of the medium and moisture in the pore space. To account for the longer diffusion paths, the effective diffusion coefficient is commonly expressed as

$$D = \frac{D_o \theta_a}{\tau} \tag{2}$$

where

D_o = free-air diffusion coefficient (l^2/t)

θ_a = air-filled porosity of soil (l^3/l^3)

τ = tortuosity value for the medium (dimensionless).

In this case, the tortuosity is a number equal to or greater than one. Substituting Equation (2) into Equation (3) provides an expression for flux *(F)* as a function of tortuosity:

$$F = \frac{D_o \theta_a C_g}{\tau} \quad . \tag{3}$$

Solving for the tortuosity *(τ)* in Equation (3) yields

$$\tau = \frac{D_o \theta_a C_g}{F} \quad . \tag{4}$$

Having a data source for all variables required for solving this equation is necessary to solve for the tortuosity value in Equation (4). The value for flux *(F)* was obtained from data collected in the field by the flux chamber unit. The concentration gradient *(C_g)* was obtained by analyzing soil gas samples collected at depths of 30 and 15 in. Air filled porosity *(θ_a)* was obtained using moisture content and porosity data collected during previous studies of surface soil in the SDA. The free air diffusion coefficient *(D_o)* was found in Lide (1995).

3.1.1 Determining Flux Using the Flux Chamber Unit

As discussed in Section 2, the flux chamber unit is a trailer-portable solar powered apparatus equipped with a standard EPA flux chamber assembly. Filtered sweep air (i.e., ambient air) is pumped into the chamber at a constant rate of approximately 1.5 L/minute (1.6 qt/minute). Sample air is extracted from the chamber at a constant rate of approximately 0.5 L/minute (0.5 qt/minute). Excess sweep air is vented through a penetration in the chamber. Both the inlet sweep air and outlet sample air pass through respective nondispersive infrared CO_2 sensors. Data, including battery voltage, temperatures, flow rates, barometric pressure, and CO_2 concentrations, are logged every 70 minutes by a Campbell Scientific 23X datalogger.

As the name implies, the flux chamber unit was used to obtain the flux of CO_2 emanating from strategic locations in the SDA. The flux values *(F)* for CO_2 provide site-specific data values to plug into Equation (4). The flux value was calculated based on the schematic mass balance illustrated in Figure 6 and the calculation that follows, assuming steady state conditions:

$$M_{in} = M_{out} \tag{5}$$

where

M_{in} = mass of CO_2 entering the flux chamber (m/t)

M_{out} = mass of CO_2 exiting the flux chamber (m/t).

Based on the schematic mass balance represented in Figure 6, M_{in} and M_{out} were determined as follows:

$$M_{in} = \left(Q_{swp} * C_{in}\right) + M_Q \quad . \tag{6}$$

$$M_{out} = \left(Q_{smpl} * C_{out}\right) + \left(Q_{vent} * C_{out}\right) \quad . \tag{7}$$

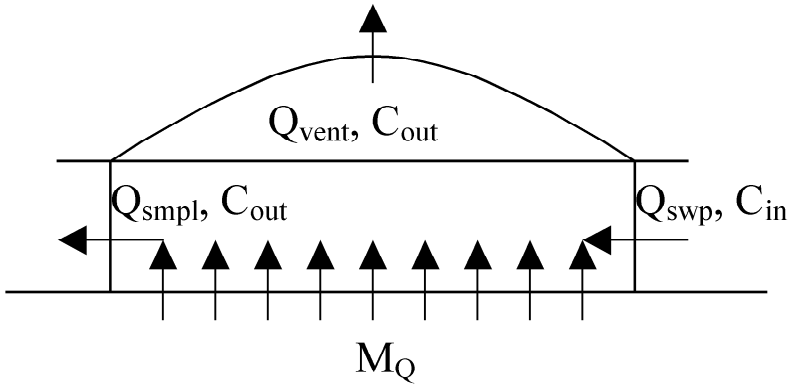

Figure 6. Schematic representation of the mass balance of CO_2 within the flux chamber.

Substituting Equations (6) and (7) into Equation (5) gives the following:

$$\left(Q_{swp} * C_{in}\right) + M_Q = \left(Q_{smpl} * C_{out}\right) + \left(Q_{vent} * C_{out}\right) \tag{8}$$

where

Q_{swp} = volumetric air flow rate entering the flux chamber (sweep air) (l^3/t)

C_{in} = ambient CO_2 concentration in sweep air (m/L^3)

M_Q = CO_2 mass entering the flux chamber through the soil surface (m/t)

Q_{smpl} = volumetric air flow rate exiting the flux chamber through the sample port (l^3/t)

C_{out} = CO_2 concentration exiting the flux chamber (m/L^3)

Q_{vent} = volumetric air flow rate exiting flux chamber through chamber penetration (l^3/t).

Solving for M_Q gives:

$$M_Q = C_{out}\left(Q_{smpl} + Q_{vent}\right) - \left(Q_{swp} * C_{in}\right) \ . \tag{9}$$

Assuming that there is no air flow into the flux chamber through the soil surface, the following is true:

$$\left(Q_{smpl} + Q_{vent}\right) = Q_{swp} \ . \tag{10}$$

Substituting Equation (10) into Equation (9) yields

$$M_Q = Q_{swp}\left(C_{out} - C_{in}\right) \ . \tag{11}$$

By defining ΔC_F as the change between the incoming concentration and the outgoing concentration within the flux chamber, the above equation can be rewritten as:

$$M_Q = Q_{swp}\left(\Delta C_F\right) \quad . \tag{12}$$

The flux value *(F)* is defined as the mass of a constituent that diffuses through a unit area of soil over a unit of time. Based on this definition, flux is determined by the following series of equations:

$$F = \frac{M_Q}{A} \tag{13}$$

where

F = mass flow of CO_2 diffusing through soil per unit area ($m/L^2/t$)

A = surface area of soil encompassed by the flux chamber (l^2).

Substituting Equation (12) into Equation (13) gives the following equation for determining the flux value based on data collected from the flux chamber unit:

$$F = \frac{Q_{swp}\left(\Delta C_F\right)}{A} \quad . \tag{14}$$

3.1.2 Tortuosity Equation

Substituting Equation (14) into Equation (4) gives the expression for tortuosity:

$$\tau = \frac{AD_o\theta_a C_g}{Q_{swp}\left(\Delta C_F\right)} \quad . \tag{15}$$

3.2 Data Collection

To calculate the tortuosity factor using Equation (15), data values for the variables must be determined. Data from the flux chamber unit can be used to determine all but two of the values required for the calculation. These two values include the air-filled porosity value *(0_a)* and the concentration gradient *(C_g)*.

3.2.1 Determination of Air-Filled Porosity

The air-filled porosity *(θ_a)* was estimated from existing porosity and moisture content data for SDA surface sediments. Ideally, the most representative data would come from samples taken near the deployment locations when the flux chamber was operating (i.e., collecting data). However, this was not feasible; therefore, existing data were used for SDA sediments.

McCarthy and McElroy (1995) made a compilation of hydraulic characterization data for surficial sediments and interbeds at the SDA collected before 1995. A significant source of data collected since 1995 is contained in Bishop (1998). Though other sources of data may be available, the data in these two references are sufficient for this study.

This study was limited to an examination of data representative of the conditions present where and when the flux chamber measurements were taken. These conditions included the following:

- Shallow soil—Surface fluxes are influenced primarily by conditions at shallow depths. The concentration gradient used in the flux calculations was based on measurements less than 3 ft (0.9 m) deep.

- Disturbed soil (overburden materials)—The flux chamber was placed on overburden materials over waste pits. The overburden soil was disturbed clay-loam soil native to the SDA or brought in from nearby playas.

- Seasonal and environmental circumstances—Flux measurements were made during the time of year when shallow moisture contents are lowest and during a multiyear low-precipitation (i.e., dry) cycle.

3.2.1.1 Porosity. Some of the most appropriate data for estimating porosity of shallow, disturbed soil at the SDA comes from studies by Borghese (1988) and Schakofsky (1993). Data from these reports are contained in McCarthy and McElroy (1995). Borghese analyzed shallow soil samples from disturbed sites on the SDA. Schakofsky studied shallow soil from disturbed (i.e., a simulated waste trench) and undisturbed sites near the SDA. Table 1 shows the porosity values from the two studies for disturbed samples less than 5 ft (1.5 m) deep. Though the data from disturbed samples are of greatest interest, the undisturbed samples less than 5 ft (1.5 m) deep from Schakofsky's study also are shown because they help define a type of lower limit for disturbed samples. The numbers at the bottom of the Table 1 are the average and standard deviations from each sample set.

The Schakofsky disturbed samples had a slightly higher average porosity than the Borghese disturbed samples, perhaps because the Schakofsky samples were more recently disturbed; therefore, less settling and compaction had occurred. Nevertheless, the average values from all sample sets (even the undisturbed values from Schakofsky) were quite close. Because the Borghese soil is closer to that from the flux chamber locations in terms of location and length of time disturbed, the Borghese numbers (48% with a standard deviation of 2.5%) were used to calculate air-filled porosity.

Table 1. Porosity data for shallow sediments on and near the Subsurface Disposal Area.

Borghese (Disturbed) (%)	Schakofsky (Freshly Disturbed) (%)	Schakofsky (Undisturbed) (%)
51	50	47
47	53	47
51	43	46
47	49	44
47	53	48
47	50	46
43	55	45
51	56	45
47	50	45
47	—	—
Average = 48	Average = 51	Average = 46
Standard Deviation = 2.5	Standard Deviation = 3.9	Standard Deviation = 1.3

3.2.1.2 Moisture Content. Determining an appropriate value to use for the flux chamber study is simplified by the fact that conditions were very dry during the time when the flux measurements were made. The flux measurements were made in late summer and autumn, which is typically the driest part of the year for shallow sediments as determined from moisture logs using a neutron probe (Bishop 1998). The neutron probe readings were taken in several access tubes installed in and around the SDA. Readings were made routinely over a 3-year period from 1994 to 1996. These readings show that moisture contents in the shallow sediments are lowest in late summer and fall. In addition, precipitation totals in 2000 and 2001 were very low, which added to the very dry conditions. The combination of the time of year and the low precipitation totals most likely reduced moisture contents to residual or irreducible levels.

Typically, moisture contents in shallow sediments (less than 5 ft [1.5 m]) in late summer and autumn decrease to a seasonal low of 10 to 20%, and more commonly in the 10 to 15% range. This is near the irreducible soil water content of 11 to 12%, as calculated by Anderson et al. (1987) for a disturbed plot of INEEL soil. Given that the flux chamber measurements were made during a dry time of the year and during a dry climatic cycle, it is reasonable to assume that the moisture contents were at or near the irreducible level. Therefore, a value of 12% was used and a standard deviation of 4% was assumed.

3.2.1.3 Air Porosity. The air-filled porosity was determined by subtracting the moisture content value (12% standard deviation 4%) from the porosity value (48% standard deviation 2.5%) to get a value of 36% with a standard deviation of 4.7%.

3.2.2 Determination of Concentration Gradient

The concentration gradient *(C_g)* was determined using site-specific field data. Multiple vapor samples were collected from depths of 15 and 30 in. (38 and 76 cm) at each deployment location while the flux chamber unit was collecting data. For each sampling event, gradient values were determined from 30 to 15 in. (76 and 38 cm) and from 15 in. (38 cm) to the surface of the soil. The average of these site-specific values was used in calculations for determining the tortuosity factor.

3.3 Flux Chamber Unit Deployment

3.3.1 Deployment Locations and Unit Settings

To collect defensible data for this study, the flux chamber was deployed at three different locations inside the SDA as show in Figure 7. The locations were chosen based on assumed locations of VOC burial (Miller and Varvel 2001), multiple pit locations, and the ability to deploy the flux chamber unit for extended periods without impeding other operations in the SDA. It also was desirable to deploy the flux chamber over areas with expected elevated CO_2 concentrations to decrease the error associated with subsequent calculations.

The flux chamber unit was programmed to collect data every 70 minutes and was deployed at each location for a period of 3 weeks. The last 2 weeks of data from each location were used in this study to allow for equilibration of the unit. Summary information of flux chamber data and concentration gradient data is provided in Appendices A and B, respectively.

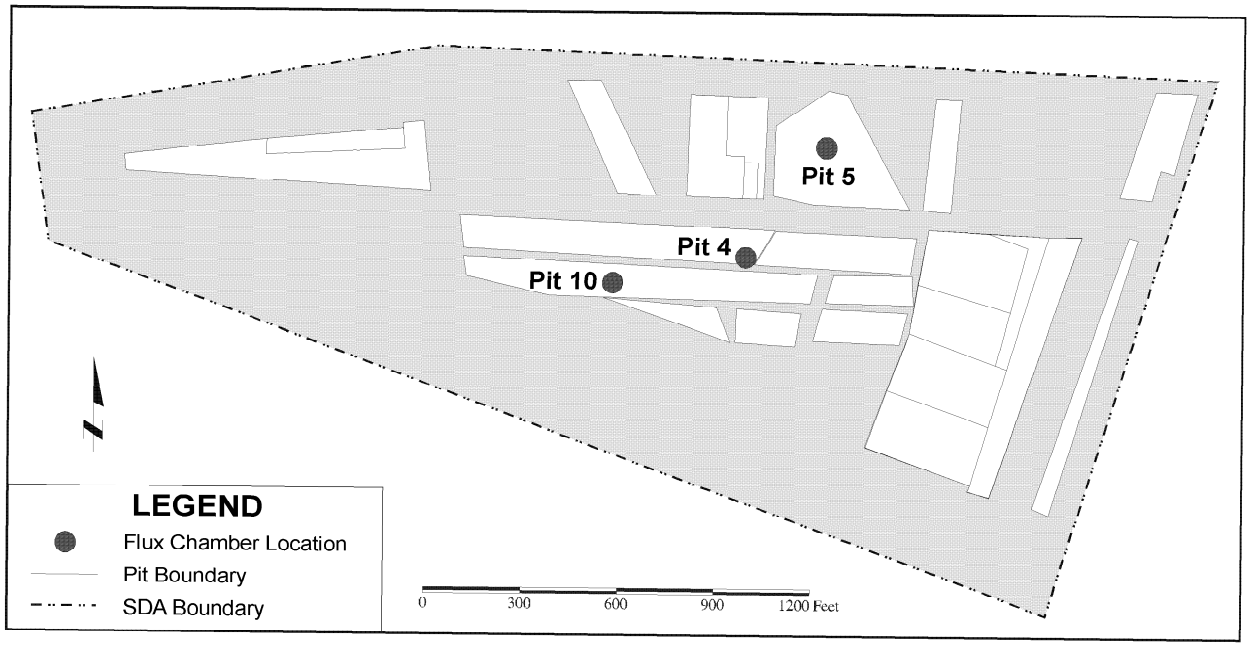

Figure 7. Flux chamber deployment locations in Pits 4, 5, and 10 at the Subsurface Disposal Area.

4. ESTIMATIONS OF TORTUOSITY FACTOR

4.1 Estimations Using Flux Chamber Unit Data

This section provides the calculations of tortuosity factors and standard deviation for each of the three deployment locations (i.e., Pits 4, 5, and 10) in the SDA. Equation (15) is used for the tortuosity calculations, and error propagation methods were derived from NCRP (1985). The following variables are consistent for each calculation:

- Surface area (A) = 0.13 m^2.

  Explanation: This value was determined by measuring the diameter of the flux chamber base (16.14 in. [0.41 m]) and calculating the coverage area of the chamber. The standard deviation for this value was assumed to be negligible.

- Free air diffusivity (D_o) = 9.6E-04 m^2/minute.

  Explanation: This value is the binary diffusion coefficient for CO_2 in the air at 293.15 K (68°F) (Lide 1995). Though soil temperatures are generally less than 293.15 K (68°F), this value is assumed to be valid for these calculations. The standard deviation for this value was assumed to be negligible.

- Air-filled porosity (θ_a) = 0.36.

  Explanation: See Section 3.2.1. Standard deviation = 4.7.

The remaining variables have values that are site specific and are defined in their respective sections.

4.1.1 Tortuosity Factor Determination for Pit 10

The following values are specific to the Pit 10 location over which the flux chamber was deployed.

- Carbon dioxide concentration gradient (C_{g10}) = 5,310 ppmv/m.

  Explanation: This value was determined by using field data and the methods listed in Table 2. Samples were collected four times throughout the deployment interval over Pit 10. The standard deviation for this value is 3,150 ppmv/m.

- Sweep air-flow rate (Q_{swp10}) = 1.46E-03 m^3/minute.

  Explanation: This value was determined by taking the average of sweep flow values collected while the flux chamber unit was operating over Pit 10. The standard deviation of this value was determined to be 4.4E-05 m^3/minute.

- Carbon dioxide concentration change in flux chamber (ΔC_{f10}) = 35.4 ppmv.

  Explanation: This value was determined from the data collected by the flux chamber unit. The difference was taken between respective sample air CO_2 concentrations and sweep air CO_2 concentrations. The average of these values was found to be 35.4 ppmv with a standard deviation of 34.3 ppmv.

Table 2. Shallow vapor data results from the Pit 10 deployment location.

Column A	Column B	Column C	Column D		
Sample Depth 1 (m)	Sample Depth 2 (m)	Sample CO_2 Concentration 1 (ppmv)	Sample CO_2 Concentration 2 (ppmv)	Calculation Based on Column Values	C_g (ppmv/m)
0.762	0.381	1,877.2	928.5	(C-D)/(A-B)	2,490.0
0.381	0.0	928.5	444.5	(C-D)/(A-B)	1,270.3
0.762	0.381	4,204.0	2,482.5	(C-D)/(A-B)	4,518.4
0.381	0.0	2,482.5	456.3	(C-D)/(A-B)	5,318.1
0.762	0.381	4,095.3	2,129.4	(C-D)/(A-B)	5,159.8
0.381	0.0	2,129.4	424.7	(C-D)/(A-B)	4,474.3
0.762	0.381	7,780.6	4,815.0	(C-D)/(A-B)	7,783.7
0.381	0.0	4,815.0	450.3	(C-D)/(A-B)	11,455.9
				Average =	5,308.8
				Standard deviation =	3,151.2

Substituting the previously defined site-specific values into Equation (15) yields the following tortuosity factor for the Pit 10 location:

$$\tau_{10} = \frac{0.13 m^2 * 9.6E-04 \frac{m^2}{\min} * 0.36 * 5310 \frac{ppmv}{m}}{1.46E-03 \frac{m^3}{\min} * 35.4\, ppmv}$$

$$\tau_{10} = 4.6 \quad . \tag{16}$$

The standard deviation for τ_{10} was determined through the following equation:

$$STD\tau_{10} = \sqrt{\left(\frac{(VarA)}{(A)^2} + \frac{(VarD_o)}{(D_o)^2} + \frac{(Var\theta_a)}{(\theta_a)^2} + \frac{(VarC_{g10})}{(C_{g10})^2} + \frac{(VarQ_{swp10})}{(Q_{swp10})^2} + \frac{(Var\Delta C_{f10})}{(\Delta C_{f10})^2} \right) * (\tau_{10})^2} \tag{17}$$

where

$VarA$ = variance of A, which is 0

$VarD_o$ = variance of D_o, which is 0

$Var\theta_a$ = variance of θ_a, which is 2.2E-03

$VarC_{g10}$ = variance of C_{g10}, which is 9.9E+06

$VarQ_{swp10}$ = variance of Q_{swp10}, which is 1.9E-09

$Var\Delta C_{f10}$ = variance of ΔC_{f10}, which is 1.2E+03.

Substituting the above values into Equation (17) yields the following:

$$STD\tau_{10} = \sqrt{\left(\frac{(0)}{(0.13)^2} + \frac{(0)}{(9.6E-04)^2} + \frac{(2.2E-03)}{(0.36)^2} + \frac{(9.9E+06)}{(5310)^2} + \frac{(1.9E-09)}{(1.46E-03)^2} + \frac{(1.2E+03)}{(35.4)^2} \right) * (4.6)^2}$$

$$STD\tau_{10} = \sqrt{28.1}$$

$$STD\tau_{10} = 5.3 \quad . \tag{18}$$

Thus, the tortuosity factor over Pit 10 is 4.6 (standard deviation = 5.3).

4.1.2 Tortuosity Factor Determination for Pit 5

The values provided below are specific to the Pit 5 location over which the flux chamber was deployed.

- Concentration gradient (C_{g5}) = 8,810 ppmv/m.

  Explanation: This value was determined using field data and the methods listed in Table 3. Samples were collected four times throughout the deployment interval over Pit 5. The standard deviation for this value is 3,010 ppmv.

- Sweep air flow rate (Q_{swp5}) = 1.47E-03 m^3/minute.

  Explanation: This value was determined by taking the average of sweep air-flow rate values collected while the flux chamber unit was operating over Pit 5. The standard deviation of this value was determined to be 5.6E-05 m^3/minute.

- Carbon dioxide concentration change in flux chamber (ΔC_{f5}) = 94.6 ppmv.

  Explanation: This value was determined from the data collected by the flux chamber unit. The difference was taken between respective sample air CO_2 concentrations and sweep air CO_2 concentrations. The average of these values was found to be 94.6 ppmv with a standard deviation of 39.6 ppmv.

Table 3. Shallow vapor data results from the Pit 5 deployment location.

Column A	Column B	Column C	Column D		
Sample Depth 1 (m)	Sample Depth 2 (m)	Sample CO_2 Concentration 1 (ppmv)	Sample CO_2 Concentration 2 (ppmv)	Calculation Based on Column Values	C_g (ppmv/m)
0.762	0.381	9,446.7	5,112.5	(C-D)/(A-B)	11,375.9
0.381	0.0	5,112.5	413.2	(C-D)/(A-B)	12,334.1
0.762	0.381	4,343.9	2,249.0	(C-D)/(A-B)	5,498.4
0.381	0.0	2,249.0	435.0	(C-D)/(A-B)	4,761.2
0.762	0.381	6,870.1	4,679.5	(C-D)/(A-B)	5,749.6
0.381	0.0	4,679.5	436.1	(C-D)/(A-B)	11,137.5
0.762	0.381	7,921.8	4,346.5	(C-D)/(A-B)	9,384.0
0.381	0.0	4,346.5	431.8	(C-D)/(A-B)	10,274.8
				Average =	8,814.4
				Standard deviation =	3,014.8

Substituting the previously defined site-specific values into Equation (15) yields the following tortuosity factor for the Pit 5 location:

$$\tau_5 = \frac{0.13 m^2 * 9.6E-04 \frac{m^2}{\min} * 0.36 * 8810 \frac{ppmv}{m}}{1.47E-03 \frac{m^3}{\min} * 94.6 ppmv}$$

$$\tau_5 = 2.8 \quad . \tag{19}$$

The standard deviation for τ_5 was determined through the following equation:

$$STD\tau_5 = \sqrt{\left(\frac{(VarA)}{(A)^2} + \frac{(VarD_o)}{(D_o)^2} + \frac{(Var\theta_a)}{(\theta_a)^2} + \frac{(VarC_{g5})}{(C_{g5})^2} + \frac{(VarQ_{swp5})}{(Q_{swp5})^2} + \frac{(Var\Delta C_{f5})}{(\Delta C_{f5})^2} \right) * (\tau_5)^2} \tag{20}$$

where

$VarA$ = variance of A, which is 0

$VarD_o$ = variance of D_o, which is 0

$Var\theta_a$ = variance of θ_a, which is 2.2E-03

$VarC_{g5}$ = variance of C_{g5}, which is 9.1E+06

$VarQ_{swp5}$ = variance of Q_{swp5}, which is 3.1E-09

$Var\Delta C_{f5}$ = variance of ΔC_{f5}, which is 1.6E+03.

Substituting the above values into Equation (20) yields the following:

$$STD\tau_5 = \sqrt{\left(\frac{(0)}{(0.13)^2} + \frac{(0)}{(9.6E-04)^2} + \frac{(2.2E-03)}{(0.36)^2} + \frac{(9.1E+06)}{(8810)^2} + \frac{(3.1E-09)}{(1.47E-03)^2} + \frac{(1.6E+03)}{(96.4)^2} \right) * (2.8)^2}$$

$$STD\tau_5 = \sqrt{2.4}$$

$$STD\tau_5 = 1.5 \quad . \tag{21}$$

Thus, the tortuosity factor over Pit 5 is 2.8 (standard deviation = 1.5).

4.1.3 Tortuosity Factor Determination for Pit 4

The values described below are specific to the Pit 4 location over which the flux chamber was deployed.

- Concentration gradient (C_{g4}) = 2,490 ppmv/m.

  Explanation: This value was determined using field data and the methods listed in Table 4. Samples were collected four times throughout the deployment interval over Pit 4. The standard deviation for this value is 510 ppmv.

- Sweep air-flow rate (Q_{swp4}) = 1.38E-03 m^3/minute.

  Explanation: This value was determined by taking the average of sweep air-flow rate values collected while the flux chamber unit was operating over Pit 4. The standard deviation of this value was determined to be 7.6E-05 m^3/minute.

- Carbon dioxide concentration change in flux chamber (ΔC_{f4}) = 25.0 ppmv.

  Explanation: This value was determined from the data collected by the flux chamber unit. The difference was taken between respective sample air CO_2 concentrations and sweep air CO_2 concentrations. The average of these values was found to be 25.0 ppmv with a standard deviation of 13.8 ppmv.

Table 4. Shallow vapor data results from the Pit 4 deployment location.

Column A	Column B	Column C	Column D		
Sample Depth 1 (m)	Sample Depth 2 (m)	Sample CO_2 Concentration 1 (ppmv)	Sample CO_2 Concentration 2 (ppmv)	Calculation Based on Column Values	C_g (ppmv/m)
0.762	0.381	2,767.8	1,807.2	(C-D)/(A-B)	2,521.3
0.381	0.0	1,807.2	431.8	(C-D)/(A-B)	3,610.0
0.762	0.381	2,342.8	1,300.5	(C-D)/(A-B)	2,735.7
0.381	0.0	1,300.5	424.8	(C-D)/(A-B)	2,298.4
0.762	0.381	2,089.7	1,258.0	(C-D)/(A-B)	2,182.9
0.381	0.0	1,258.0	416.4	(C-D)/(A-B)	2,208.9
0.762	0.381	2,090.6	1,148.4	(C-D)/(A-B)	2,473.0
0.381	0.0	1,148.4	416.1	(C-D)/(A-B)	1,922.0
				Average =	2,494.0
				Standard deviation =	513.9

Substituting the previously defined site-specific values into Equation (15) yields the following tortuosity factor for the Pit 4 location:

$$\tau_4 = \frac{0.13 m^2 * 9.6E-04 \frac{m^2}{\min} * 0.36 * 2490 \frac{ppmv}{m}}{1.38E-03 \frac{m^3}{\min} * 25.0\, ppmv}$$

$$\tau_5 = 3.2 \quad . \tag{22}$$

The standard deviation for τ_4 was determined through the following equation:

$$STD\tau_4 = \sqrt{\left(\frac{(VarA)}{(A)^2} + \frac{(VarD_o)}{(D_o)^2} + \frac{(Var\theta_a)}{(\theta_a)^2} + \frac{(VarC_{g4})}{(C_{g4})^2} + \frac{(VarQ_{swp4})}{(Q_{swp4})^2} + \frac{(Var\Delta C_{f4})}{(\Delta C_{f4})^2} \right) * (\tau_4)^2} \tag{23}$$

where

$VarA$ = variance of A, which is 0

$VarD_o$ = variance of D_o, which is 0

$Var\theta_a$ = variance of θ_a, which is 2.2E-03

$VarC_{g4}$ = variance of C_{g4}, which is 2.6E+05

$VarQ_{swp4}$ = variance of Q_{swp4}, which is 5.8E-09

$Var\Delta C_{f4}$ = variance of ΔC_{f4}, which is 1.9E+02.

Substituting the above values into Equation (23) yields the following:

$$STD\tau_5 = \sqrt{\left(\frac{(0)}{(0.13)^2} + \frac{(0)}{(9.6E-04)^2} + \frac{(2.2E-03)}{(0.36)^2} + \frac{(2.6E+05)}{(2490)^2} + \frac{(5.8E-09)}{(1.38E-03)^2} + \frac{(1.9E+02)}{(25.0)^2} \right) * (3.2)^2}$$

$$STD\tau_5 = \sqrt{3.7}$$

$$STD\tau_5 = 1.9 \quad . \tag{24}$$

Thus, the tortuosity factor over Pit 4 is 3.2 (standard deviation = 1.9).

4.1.4 Explanation of Tortuosity Factor Error

The primary factors contributing to the relatively large standard deviation values are variance in the subsurface concentration gradient *(C_g)* and variance in the difference between the incoming and outgoing CO_2 concentrations within the flux chamber *(ΔC_F)*. This is likely the result of fluctuations in barometric pressure, which was not accounted for in the analysis. Figure 8 shows a diurnal pattern of changes in ΔC_F, likely because of barometric pumping of air in the soil cover. The diurnal fluctuations are caused by temperature changes brought about by the daily heating and cooling of the earth. Though similar variations in C_g may have occurred as a result of barometric pumping, the variations could not be detected without increasing the sample frequency.

It also is important to note that for this study, CO_2 was assumed to be diffusing from a large areal source deeper than 30 in. (76 cm) in depth. The CO_2 generation rate from waste buried in the Pits was assumed to be relatively constant and much larger than any natural production elsewhere in the soil, such as from plant roots and microbial consumption of organic material within the overburden soil. This appears to be a good assumption because the measured CO_2 concentrations in the soil cover were many times greater than atmospheric concentrations.

The calculated tortuosity factors using the flux chamber data were assumed to be relatively good estimates for the referenced locations, conditions, and purpose of their use. The moderately large standard deviations are most likely attributed to advective breathing of air in and out of the soil as a result of diurnal atmospheric pressure and temperature changes. While this phenomenon would increase the standard deviation values, the mean tortuosity value would remain relatively constant. Regardless, the standard deviation of each value takes into account any external factors such as advection and an upper and lower estimate can be determined for the tortuosity factor based on diffusion using the respective standard deviation of each value.

4.2 Estimations Using Theoretical and Empirical Equations

Theoretical and empirical equations for determining the tortuosity factor were used to make comparisons with the tortuosity factor values calculated in the previous section. The equations used for this comparison were derived using Millington (1959), Currie (1970), and Albertson (1979) methods (Weeks 1982). The Millington equation is based on theoretical pore sizes while the other two equations were empirically derived from laboratory data. The equations that follow were used in determining the tortuosity factors for each method.

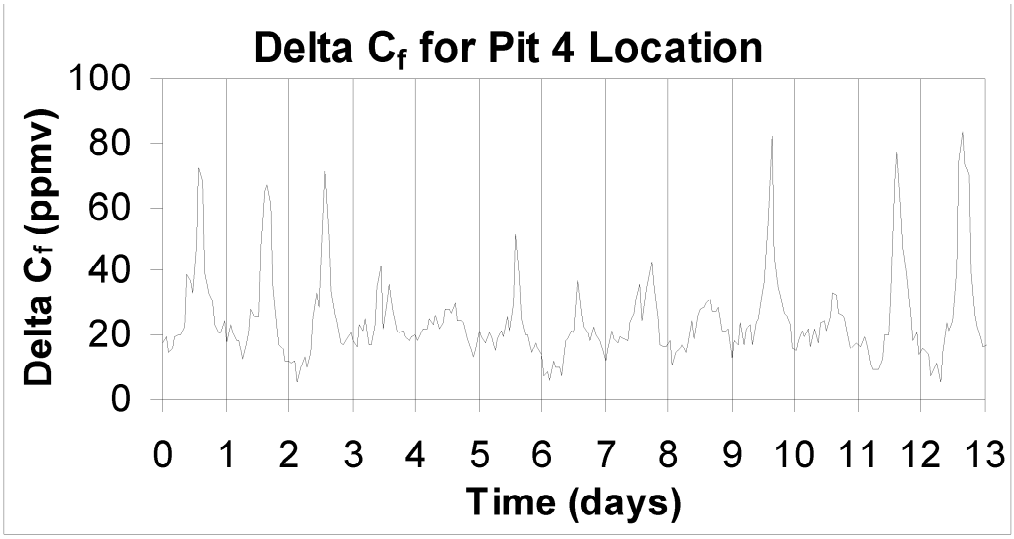

Figure 8. Chart displaying diurnal fluctuations in ΔC_F over Pit 4.

4.2.1 Millington (1959) Method

$$\tau_M = \left(\frac{1}{\theta_a}\right)^{0.333} * \left(\frac{\theta_T}{\theta_a}\right)^2 \quad (25)$$

where

θ_T = total porosity (0.48 standard deviation 0.025)

θ_a = air-filled porosity (0.36 standard deviation 0.047).

Substituting the above values into Equation (25) yields:

$$\tau_M = \left(\frac{1}{0.36}\right)^{0.333} * \left(\frac{0.48}{0.36}\right)^2$$

$$\tau_M = 2.5 \text{ standard deviation } 0.54 \ . \quad (26)$$

Therefore, assuming the Millington Method is correct, based on a standard normal distribution, a 95% probability exists that the true tortuosity value lies within the following range:

$$\tau_M = 1.8 - 3.4 \quad . \tag{27}$$

4.2.2 Currie (1970) Method

$$\tau_C = \left(\frac{1}{\theta_T}\right)^{0.5} * \left(\frac{\theta_T}{\theta_a}\right)^4 \quad . \tag{28}$$

Substituting the previously defined values into Equation (28) yields

$$\tau_C = \left(\frac{1}{0.48}\right)^{0.5} * \left(\frac{0.48}{0.36}\right)^4$$

$$\tau_C = 4.6 \text{ standard deviation } 1.3 \quad . \tag{29}$$

Thus, assuming the Currie Method is correct, based on a standard normal distribution, a 95% probability exists that the true tortuosity value lies within the following range:

$$\tau_C = 2.9 - 6.2 \quad . \tag{30}$$

4.2.3 Albertson (1979) Method

$$\tau_A = \frac{1}{\left(\frac{0.777 * \theta_a}{\theta_T}\right) - 0.274} \quad . \tag{31}$$

Substituting the previously defined values into Equation (31) yields

$$\tau_A = \frac{1}{\left(\frac{0.777 * 0.36}{0.48}\right) - 0.274}$$

$$\tau_A = 3.2 \text{ standard deviation } 0.45 \quad . \tag{32}$$

Therefore, assuming the Albertson Method is correct, based on a standard normal distribution, a 95% probability exists that the true tortuosity value lies within the following range:

$$\tau_A = 2.6 - 3.8 \quad . \tag{33}$$

4.3 Summary of Calculated Tortuosity Factors

The values for the tortuosity factor, which were calculated using the flux chamber unit data, relate closely to values calculated with the theoretical and empirical equations in Section 4.2.

Values calculated for the tortuosity factor of soil in the SDA are listed in Table 5, as well as 95% confidence ranges for each calculated value. With the exception of the range for Pit 10, the tortuosity factors calculated from flux chamber data appear to be reasonable and comparable to values and ranges calculated using theoretical and empirical formulae.

Table 5. Calculated tortuosity factors using flux chamber unit data and theoretical and empirical formulas.

Method	Location	Tortuosity Factor	95% Confidence Range[a]
Flux chamber unit data	Pit 10 of the SDA	4.6	0 to 11.4
Flux chamber unit data	Pit 5 of the SDA	2.8	0.9 to 4.7
Flux chamber unit data	Pit 4 of the SDA	3.2	0.8 to 5.6
Millington (1959)	SDA (general)	2.5	1.8 to 3.4[b]
Currie (1970)	SDA (general)	4.6	2.9 to 6.2[b]
Albertson (1979)	SDA (general)	3.2	2.6 to 3.8[b]

a. The values show were calculated based on a standard normal distribution.
b. The value shown incorporates the assumption that the method used is correct.

5. CONCLUSIONS AND RECOMMENDATIONS

The determination of a site-specific tortuosity factor for soil in the SDA provided results consistent with existing theoretical and empirical equations. The range of mean values for the tortuosity factor for each deployment location in the SDA was determined to be 2.8 to 4.6, while empirical and theoretical equations produced a range of 2.5 to 4.6.

While the ranges of these results may seem relatively large, they provide important information for fate and transport models, which in the past used tortuosity factors from two to four times larger than those calculated in Table 5 (Magnuson and Sondrup 1998; Sondrup 1998). The results of this study show that the tortuosity factors employed by those models may be overestimated. It should be noted, however, that those large tortuosity factors were compensating for an underestimated source term and were representative of a much wider range of moisture content. It is important to note that tortuosity factors increase in a nonlinear fashion with increasing moisture content. Nevertheless, the information from this study will improve fate and transport modeling efforts by providing a tortuosity factor that is based on site-specific data rather than an assumed value.

If a more accurate value for the tortuosity factor is necessary, a more rigorous evaluation of barometric effects is recommended. Two additional CO_2 sensors and pump systems should be added to the flux chamber unit. The additional sensors and pump systems would collect CO_2 concentration gradient data concurrent with other collected data. This in turn would reduce the error associated with the current method of determining the concentration gradient while possibly decreasing the deviation of data attributed to advection. In addition, site-specific soil samples should be analyzed for total porosity and soil moisture content data should be collected concurrent with flux data.

6. REFERENCES

Albertson, M., 1979, "Carbon Dioxide Balance in the Gas-Filled Part of the Unsaturated Zone, Demonstrated at the Podzol (in German)," *A. Pflanzenernaehr. Bodenkd*, Vol. 142, pp. 39–56.

Anderson, J. E., M. L. Shumar, N. L. Toft, and R. S. Nowak, 1987, "Control of Soil Water Balance by Sagebrush and Three Perennial Grasses in a Cold-Desert Environment," *Arid Soil Research and Rehabilitation*, Vol. 1, pp. 229–244.

Arah, J. R. M., and B. C. Ball, 1994, "A Functional Model of Soil Porosity Used to Interpret Measurements of Gas Diffusion," *European Journal of Soil Science*, Vol. 45, pp. 135–144.

Auer, L.H., N. D. Rosenberg, K. H. Birdsell, and E.M. Whitney, 1996, "The Effects of Barometric Pumping on Contaminant Transport," *Journal of Contaminant Hydrology*, Vol. 24, pp. 145-166.

Bishop, C. W., 1998, *Soil Moisture Monitoring Results at the Radioactive Waste Management Complex of the Idaho National Engineering Laboratory, FY-96, FY-95, and FY-94*, INEEL/EXT-98/00941, Idaho National Engineering and Environmental Laboratory, Lockheed Martin Idaho Technologies Company, Idaho Falls, Idaho.

Borghese, J. V., 1988, *Hydraulic Characteristics of Soil Cover, Subsurface Disposal Area, Idaho National Engineering Laboratory*, M.S. Thesis, Department of Geology and Geological Engineering, University of Idaho, Moscow, Idaho, prepared for EG&G Idaho, Idaho Falls, Idaho, under Subcontract No. C85-110544.

Buckingham, E., 1904, *Contributions to Our Knowledge of the Aeration of Soils*, U.S. Department of Agriculture Bureau of Soils Bulletin 25, Government Printing Office, Washington.

Currie, J. A., 1970, "Movement of Gases in Soil Respiration," *Sorption and Transport Processes in Soils, SCI Monograph*, Vol. 37, Rothamsted Experimental Station, Harpenden, England.

Lide, David R., 1995, *Handbook of Chemistry and Physics 1913–1995*, 75th ed., New York, CRC Press.

Magnuson, S. O., and A. J. Sondrup, 1998, *Development, Calibration, and Predictive Results of a Simulator for Subsurface Pathway Fate and Transport of Aqueous- and Gaseous-Phase Contaminants in the Subsurface Disposal Area at the Idaho National Engineering and Environmental Laboratory*, INEEL/EXT-97-00609, Idaho National Engineering and Environmental Laboratory, Lockheed Martin Idaho Technologies Company, Idaho Falls, Idaho.

Massman, J. and D. F. Farrier, 1992, "Effects of Atmospheric Pressures on Gas Transport in the Vadose Zone," *Water Resources Research*, Vol. 28, No. 3, pp. 777-791.

McCarthy, J. M., and D. L. McElroy, 1995, *SDA Hydraulic Characterization Data Compilation: Surficial Sediments and Interbeds*, Engineering Design File ER-WAG7-71, INEL-95/130, Idaho National Engineering and Environmental Laboratory, Lockheed Martin Idaho Technologies Company, Idaho Falls, Idaho.

Miller, Eric C., and Mark D. Varvel, 2001, *Reconstructing the Past Disposal of 743-Series Waste in the Subsurface Disposal Area for Operable Unit 7-08, Organic Contamination in the Vadose Zone*, Idaho National Engineering and Environmental Laboratory, Bechtel BWXT Idaho, LLC, Idaho Falls, Idaho.

Millington, R. J., 1959, "Gas Diffusion in Porous Media," *Science*, Vol. 130.

NCRP, 1985, *A Handbook of Radioactivity Measurements Procedures*, NCRP Report No. 58, National Council of Radiation Protection and Measurements, Bethesda, Maryland.

Nilson, R. H., E. W. Peterson, K. H. Lie, N. R. Burkhard and J. R. Hears, 1991, "Atmospheric Pumping: A Mechanism Causing Vertical Transport of Contaminated Gases Through Fractured Permeable Media," *Journal of Geophysical Research*, Vol. 96, No. B13, pp. 21933–21948.

Schakofsky, S., 1993, *Changes in the Hydraulic Properties of a Soil Caused by Construction of Waste Trench at a Radioactive Waste Disposal Site*, M.S. Thesis, San Jose State University, San Jose, California.

Sondrup, A. J., 1998, *Preliminary Modeling of VOC Transport for Operable Unit 7-08, Evaluation of Increased Carbon Tetrachloride Inventory*, INEEL/EXT-2000-00849, Rev. 0, Idaho National Engineering and Environmental Laboratory, Bechtel BWXT Idaho, LLC, Idaho Falls, Idaho.

Thibodeaux, L. J., and S. T. Hwang, 1982, "Landfarming of Petroleum Wastes—Modeling the Air Emissions Problem," *Environmental Progress*, Vol. 1, No. 1, pp. 42–46.

Weeks, Edwin P., 1982, "Use of Atmospheric Fluorocarbons F-11 and F-12 to Determine the Diffusion Parameters of the Unsaturated Zone in the Southern High Plains of Texas," *Water Resources Research*, Vol. 18, No. 5, pp. 1365–1378.